Simulation and fabrication of surface-modified glass coverslips to enhance energy harvesting on indoor MOS solar cells

Gabriel O. Louzada, Fábio Izumi, Marcos N. Watanabe, and Sebastião G. dos Santos Filho

LSI/PSI/USP, University of São Paulo, Av. Prof. Luciano Gualberto, Travessa do Politécnico, nº. 158, 05508-010, São Paulo, Brasil,
e-mail: glouzada@usp.br

***Abstract*— In this work, analytical and numerical simulations of the reflectance of glass coverslips with different rough-layer thickness were carried out to establish the conditions of use as low reflectance intensifier plates for energy harvesting on indoor MOS solar cells. Reflectance simulations as a function of the wavelength were obtained for surface-modified glass coverslips over silicon (air/surface rough layer/glass/silicon) based on the refractive indices of the three regions over silicon with negligible extinction coefficients and, for silicon, with a very low value (k = 0.019). The rough layer was modeled with different thicknesses in the range of 50 to 300 nm and with an intermediate refractive index between air and glass (n = 1.25). The thickness of the glass coverslips was varied in the range of 45 μm to 160 μm with a typical bulk refractive index of 1.50. As a result, glass coverslips have been found to enhance the conversion efficiency η of light energy into electrical energy for MOS solar cells with surface reflectance higher than that of glass coverslips for indoor energy harvesting applications. The best results of glass coverslips as intensifier plates were obtained for 81.7 μm thick glasses that presented the lowest surface average reflectance in the wavelength range of 300 to 1100 nm. The one-dimensional numerical simulation using COMSOL was very close to the analytical modeling of the air/surface rough layer/glass/silicon structure. An experimental improvement of the conversion yield was observed for any glass coverslips placed on indoor MOS solar cells. Current density x voltage curves (JxV), using indoor light illumination of 11.7 mW/cm^2 at 25ºC on the sample surface, were extracted for different thicknesses of the processed glass coverslips and the main electrical parameters were obtained for the MOS photovoltaic cells such as the short circuit current (J_{sc}), the open circuit voltage (V_{oc}) and energy conversion efficiency (η). As a result, a significant increase of the indoor energy conversion efficiency was obtained for the thickness of the glass coverslip of 81.7 μm compared to those without chemical thinning (~130 μm thick), this is to say, η ≈ 5.15% against η ≈ 3.36%, respectively, which was explained by a decrease of surface reflectance of the glass coverslips in accordance with the simulation results of the rough layers.**

***Index Terms*— energy harvesting, indoor MOS solar cell, glass coverslip, low reflectance plate.**

INTRODUCTION

Nowadays, the market of indoor photovoltaics (IPV) for energy harvesting is growing rapidly aiming at the future generations of 5G and 6G telecommunications and the different future scenarios of Internet of Things (IoT), including smart homes, smart cities and smart factories, especially for innovative PV devices able to simultaneously harvest energy and receive optical wireless communication data [1, 2].

The energy conversion efficiency for outdoor commercial crystalline silicon (C-Si) solar cells reaches approximately (26.7 ± 0.5) % for incident light power density of 100 mW/cm^2 in sunny days [3-5], while indoor silicon PV devices displays powers in the mW range with energy conversion efficiency of ~ 4% - 6% [1, 2].

Metal-insulator-semiconductor (MIS) photovoltaic cell has been considered for indoor energy harvesting because it has several important characteristics for integrated circuits (ICs), such as [6-12]: i) it can be used on the same silicon substrate of the typical ICs with doping level of about $1x10^{15}cm^{-3}$, ii) it is a low-cost technology, iii) its manufacturing process is very simple, and iv) its current-voltage (I-V) characteristic is reproducible. For these devices, the charge carriers' tunnel through the potential barrier of the gate dielectrics, which requires a high control of the ultrathin film thickness in the range of 1 to 2 nm and the work function of the gate material [7, 8].

The texturization of glass surfaces in diluted hydrofluoric acid can modify the surface refractive index from ~1.5, to ~1.3. This texturized or rough layer can be controlled into the shape of inverted pyramids on the surface of the glass, which helps reduce light reflection and improve its transmission through the glass. As a result, the transmittance of the glass after the surface conditioning in diluted hydrofluoric acid allows an increase in transmittance of up to 95% in a wavelength range from 350 nm to 1500 nm and, the refractive index can be varied by controlling the time and the dilution of the hydrofluoric acid used in the process. Through adequate control of the processing conditions, it is possible to ensure that the texturized or rough layer obtained is uniform and is also consistent across the entire surface, making it ideal for use in solar and optical applications. [13, 14].

In this work, glass coverslips with thickness in the range of 70 to 108 μm were fabricated and simulated as anti-reflection covers on MOS solar cells for energy harvesting with gate dielectrics grown by rapid thermal oxidation (RTO) at 850ºC on 10 Ω.cm substrates [10-12]. Aiming to understand this conversion-efficiency improvement of the MOS solar cells, the surface reflectance of glass coverslips was simulated analytically and numerically by varying both the surface rough-layer thickness and the glass substrate thickness.

SIMULATION METHODOLOGY

A. Analytical Simulation

The analytical simulation was based on the study of coatings with multiple transparent layers (DLARC) [15], which employs an equation with multiple light interactions between the layers. In the case of three layers immersed in air, the parameters r_1, r_2, r_3, θ_1, and θ_2 are defined, taking into consideration n_0, n_1, n_2, and n_3, which are the refractive indices of air, the rough layer, the glass substrate, and silicon, respectively.

In the analytical modeling of the three layers immersed in air, Equation 1 was used to obtain the reflectance [15]:

$$R = |r^2| = \frac{r_1^2 + r_2^2 + r_3^2 + r_1^2 r_2^2 r_3^2}{1 + r_1^2 r_2^2 + r_1^2 r_3^2 + r_2^2 r_3^2} \cdots$$
$$\cdots \frac{+ 2r_1 r_2 (1 + r_3^2) cos2\theta_1 + 2r_2 r_3 (1 + r_1^2) cos2\theta_2}{+ 2r_1 r_2 (1 + r_3^2) cos2\theta_1 + 2r_2 r_3 (1 + r_1^2) cos2\theta_1} \cdots$$
$$\cdots \frac{+2r_1 r_3 cos2(\theta_1 + \theta_2) + 2r_1 r_2^2 r_3 cos2(\theta_1 - \theta_2)}{+2r_1 r_3 cos2(\theta_1 + \theta_2) + 2r_1 r_2^2 r_3 cos2(\theta_1 - \theta_2)} \quad (1)$$

The constants r_1, r_2, r_3, θ_1 and θ_2 are given by [15]:

$$r_1 = \frac{n_0 - n_1}{n_0 + n_1}, r_2 = \frac{n_1 - n_2}{n_1 + n_2}, r_3 = \frac{n_2 - n_3}{n_2 + n_3} \quad (2)$$

$$\theta_1 = \frac{2\pi n_1 t_1}{\lambda}, \ \theta_2 = \frac{2\pi n_2 t_2}{\lambda} \quad (3)$$

where t_1 and t_2 are the thicknesses of the rough layer and the glass substrate, respectively, n_0 = 1 (air), n_1 = 1.25 (rough layer), n_2 = 1.50 (glass substrate), n_3 = 3.5 (silicon) and the wavelength λ is ranging from 300 nm to 1100 nm. The extinction coefficient of silicon (k = 0.019) is neglected as it does not affect significantly, as will be shown in the one-dimensional numerical simulations using the COMSOL software [16].

The analytical calculation of the reflectance of the three-layer structure was implemented in Excel for input parameters r_1, r_2, r_3, θ_1 and θ_2, rough-layer thickness t_1 in the range of 50 to 300 nm, and glass substrate thickness t_2 in the range of 45 μm to 160 μm. The typical range of wavelengths (λ) was chosen in the range of 300 to 1100 nm (from UV to near infrared) for simulation of indoor operating environment [1, 2].

B. *COMSOL Simulation*

One-dimensional numerical simulation with COMSOL software for a three-layer system immersed in air considered the air/rough layer/glass on thick silicon substrates (5 mm) and the real and imaginary parts of the refractive index. The exact numerical simulation with COMSOL software allowed one to establish that the extinction coefficient of silicon (k = 0.019) can be neglected and does not cause substantial variation on the reflectance parameter compared to the results obtained using Equation 1.

In the simulation with COMSOL, the first objective was to obtain the reflectance of silicon as a function of the wavelength as close as possible to the reported one in literature. The internal model of COMSOL uses the "Ray Optics - Geometrical Optics" module for physical layers and interfaces, which calculates all possible paths of electromagnetic waves up to the high-frequency limit, where waves are treated as light that can undergo the effects of refraction, reflection, and diffraction over time. The specification of the contours between the different layers can be done for thin and thick films, as shown in Figure 1, where the air has an "infinite" thickness, the thick silicon layer can be specified with a thickness of a few mm (5 mm), the glass substrate with thickness in the range of 45 to 160 μm (typical values for glass coverslips), and the rough layer with a thickness of 50 to 300 nm, for taking into account the surface-texturization effect, and the possible influence of glass substrate thinning steps on the light transmission through the glass [13, 14].

Figure 1 shows the structure used in the COMSOL simulations, with the parameters of thickness employed for the air and silicon layers, as well as the ranges of the air and glass layers. The data on the refractive indices of glass and silicon were loaded from the material database available in COMSOL. In addition to the reflectance graph as a function of wavelength, it is also possible to extract absorption and transmittance graphs.

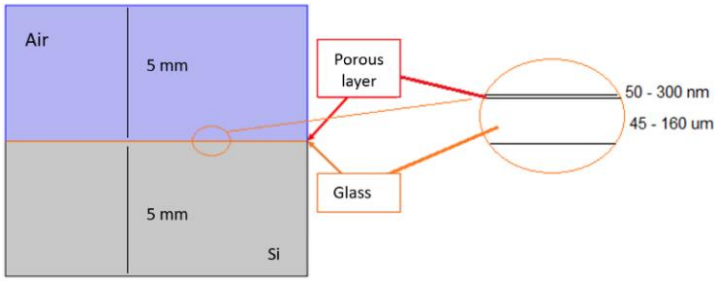

Figure 1 - Structure used in simulations with COMSOL.

EXPERIMENTAL

A. *Indoor MOS Photovoltaic cells fabrication*

Si-p substrates (100), 3 inches in diameter and resistivity of 10 Ω.cm, were used. They were chemically cleaned using a modified RCA cleaning [17] as follows: I) $16H_2O + 7H_2O_2$ (37%) + $1NH_4OH$ (38%), II) $4H_2O$ + 1HCl (38%), both at 90°C for 15 min. At the beginning of the cleaning and after each bath of the modified RCA, the silicon wafers were rinsed in deionized water (DI) for 5 min. Following, the wafers were dipped in diluted hydrofluoric acid ($80H_2O$: 1HF (49%)) for 100 s at room temperature. Finally, the silicon wafers were rinsed in DI water for 3 min.

The gate dielectrics were grown by rapid thermal oxidation (RTO) at 850ºC for 20 s in an ultra-pure mixture of nitrogen and oxygen using a gas flux of $5N_2$+$1O_2$ to obtain a dielectric thickness of 1.73 nm, as measured by a Autoel IV ellipsometer at a wavelength of 632 nm.

Aluminum was deposited by physical vapor deposition (PVD: Edwards vacuum coater auto 306) for the obtention of the gate material and back contact. Lithography was used to define the gate geometry of the MOS solar cells. The aluminum was chemically defined in a bath of $175H_3PO_4 + 70H_2O + 15HNO_3$ at a temperature of 40ºC.

B. *Glass coverslips preparation and characterization*

Square glass coverslips with an area of approximately 4 cm^2 were used. The as-received samples were previously submitted to jets of ultrapure nitrogen and their thicknesses were measured in 5 different regions (one at the center and four next to the borders) with the aid of a digital micrometer from Digimess (0-25 mm range, 0.002 mm precision and 0.001 mm resolution). The batch of glass coverslips presented average thicknesses in the range of 125 to 135 μm with standard deviations of 8 μm.

The coverslips were thinned in pairs by processing in the following baths: I) immersion in $4H_2O$: $1H_2O_2$ (37%) : $1NH_4OH$ (38%) for 15 min at 60 ºC, II) immersion for 2 h to 12 h in BOE (Buffered Oxide Etch) solution of 1HF + $6NH_4F$ with an average thinning rate of approximately (8 ± 1) μm/h,

III) again, immersion in $4H_2O$: $1H_2O_2$ (37%): $1NH_4OH$ (38%) for 15 min at 60 ºC to obtain a thin layer of SiO_2 on the coverslips, which protect them from particles that may adhere onto the surfaces. Before the first immersion and after each step (I, II and III), the glass coverslips were rinsed in deionized water (DI) for 5 min.

After the chemical thinning of the glass coverslips, the thicknesses were extracted with the aid of a digital micrometer from Digimess (0-25mm range, 0.002 mm precision and 0.001 mm resolution).

C. Electrical characterization of the indoor MOS photovoltaics cells using the glass coverlips

The IxV curves were extracted using an Agilent 4156C source measurement unit (Keysight Technologies) inside of a grounded black box to avoid external electrical interference. The equipment was programmed to apply voltage to the MOS photovoltaic cells from -2 V to 2 V with voltage step of 0.1 V. An indoor light illumination of 11.7 mW/cm^2 at 25ºC on the sample surface (3.24 cm^2 area) was performed using a 650-cd halogen lamp at a distance (d) of 9.0 cm from the gate fishbone geometry having line width (W) of 100 µm and line spacing (S) of 150 µm as illustrated in Figure 2a [10, 11].

The glass coverslips were positioned on MOS cells as shown in Figure 2b. The main photovoltaic parameters (J_{sc}, V_{oc}, FF, P_{max}, η) were extracted from the current density x voltage (JxV) and power density x voltage (PxV) characteristics.

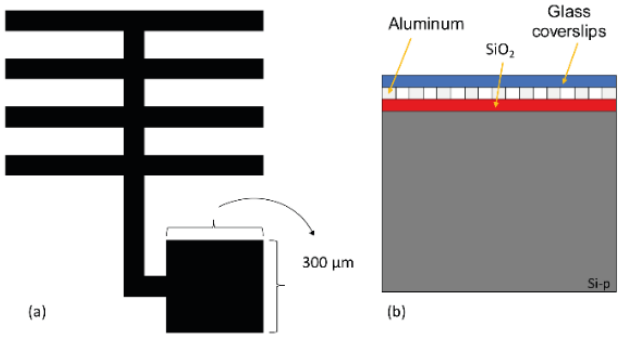

Figure 2 MOS photovoltaic cell: (a) top view and (b) profile view.

The fill factor can be obtained by [3,6,7]:

$$FF = \frac{P_{max}}{V_{oc} \cdot J_{sc}} . 100 \quad (4)$$

where P_{max} is the maximum power density (W/cm^2), V_{oc} is the open circuit voltage (V), J_{sc} is the current density (A/cm^2). The energy conversion efficiency of the cell can be obtained by [3, 10, 11]:

$$\eta = \frac{Pmax}{Pin} 100\% \quad (5)$$

where P_{in} is the light intensity density on the solar cell (W/cm^2), which is approximately 11.7 mW/cm^2 and was obtained by means of the following equation [10, 11]:

$$P_{in} = \frac{IL.f(\Delta\lambda)}{683d^2} \quad (6)$$

where IL is the light intensity in candela (cd), d is the distance between the halogen lamp and the MOS photovoltaic cell and f(Δλ) is the integrated light function by considering different penetrations for different wavelengths (λ), which is near the unitary value for MOS solar cell [10, 11].

RESULTS AND DISCUSSION

At first, COMSOL Multiphysics was employed to simulate silicon reflectance according to the procedure in the Experimental. As a result, Figure 3 shows reflectance in the range 0.31 to 0.65 for wavelength varying from 300 nm to 1100 nm according with the COMSOL. It will be shown in the following that the coverslips can decrease the surface reflectance as pointed out by analytical and numerical simulations and the energy conversion efficiency, which increases when coverslips are positioned onto the surface of MOS solar cell.

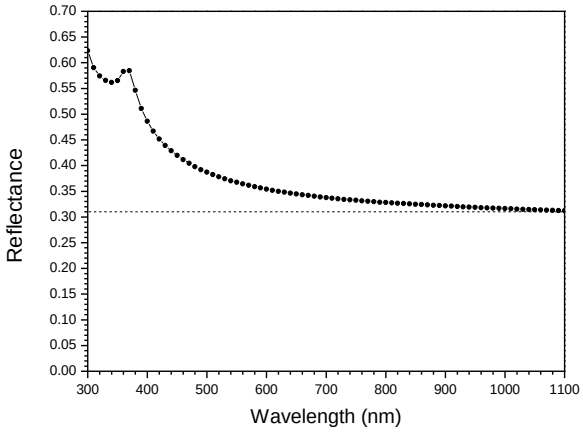

Figure 3 – Reflectance of silicon simulated with COMSOL Multiphysics in the wavelength range of 300 nm to 1100 nm.

Following, the analytical simulation was performed for the structure shown in Figure 1 with multiple transparent layers (DLARC) as described in the Experimental.

Equation 1 was solved for thickness of the rough layer in the range of 50 to 300nm (t_1 = 0, 50, 100, 150, 200, 250, and 300 nm) and glass substrate in the range of 45 to 160 µm (t_2 = 45.0, 69.6, 73.9, 81.7, 93.5, 96.8, 108.3, 130.0, and 160.0 µm) for the air/rough layer(t_1)/glass(t_2)/silicon structure.

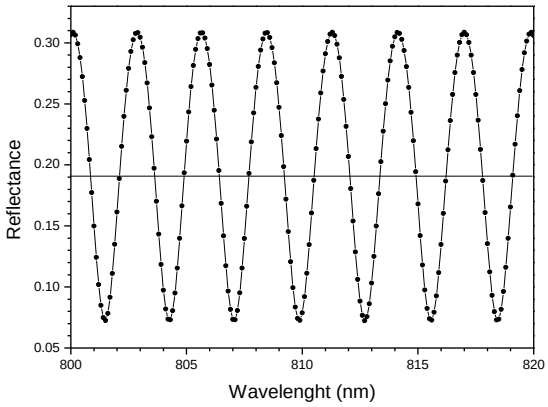

Figure 4 - Reflectance as a function of wavelength for a coverslip 81.7 µm thick without rough layer (t_1 = 0)

Reflectance is a dimensionless parameter that indicates the proportion of light intensity striking a surface which is reflected off it. Figure 4 illustrates a periodic reflectance as a function of the wavelength in the range of 800 nm to 820 nm for an 81.7 μm thick coverslip without the rough layer (t_1 = 0) placed on a thick silicon substrate (5 mm thick). It is noteworthy that, as expected, the reflectance periodicity is also observed in a broad simulated wavelength range from 300 nm to 1100 nm (not shown) with maximum at 0.3085 due to the constructive interference and the minimum at 0.0725, due to the destructive interference. For the presented periodic reflectance, the average value is 0.01905, which is 38.5% lower than the minimum silicon reflectance shown in Figure 3. For all glass thickness studied, it was observed similar average reflectance around 0.019 and a similar maximum reflectance around 0.309 from wavelike patterns for each glass thickness with different peak wavelength shifts, which do not influence the average and maximum reflectance, respectively.

Figure 5b shows the reflectance as a function of the wavelength obtained under the same conditions for a wider range of wavelengths, from UV to near infrared in the range of 300 nm to 1100 nm. In this case, it is possible to observe the decrease in the maximum value for lower wavelength in the UV range, but the average reflectance remains unchanged at ~0.175.

Figure 5a illustrates reflectance as a function of wavelength in the range of 900 nm to 1100 nm for t_1 = 50 nm and t_2 = 81.7 μm. Figure 5b shows the reflectance as a function of the wavelength obtained under the same conditions for a wider range of wavelengths, from UV to near infrared in the range of 300 nm to 1100 nm. In this case, it is possible to observe the decrease of the maximum value for lower wavelength in the UV range and the average reflectance is unchanged at ~0.175, which is lower compared with the value obtained for non-rough coverslips (t_1 = 0).

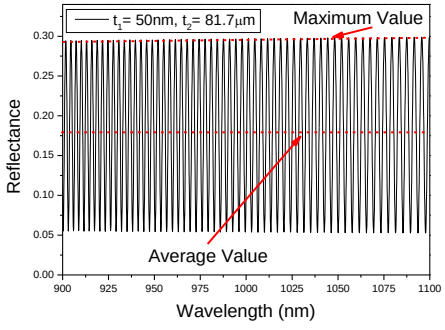

(a)

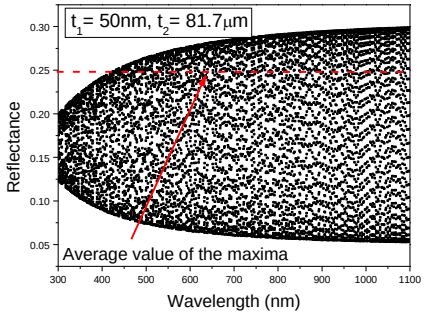

(b)

Figure 5 - Reflectance as a function of wavelength for the condition t_1= 50 nm and t_2= 81.7 um: (a) 900-1100 nm, (b) 300-1100 nm.

In Figure 5b, interference fringes are observed between the upper limit in the range 0.275 to 0.300 and a lower limit between 0.050 and 0.075 for wavelength in the range of 300 nm to 1100nm. Thus, constructive and destructive interferences are also observed, where the maximum and average values in the wavelength range are highlighted, respectively, in Figures 5a and 5b.

For practical purposes analysis, it will be considered the worst case of maximum reflectance in the wavelength range (as indicated by the red line delimiting the maximum points in Figure 5a) and the average of the maximum points (red line indicating the average value in Figure 5b). The graph in Figure 5a allows one the visualization of the reflectance maxima and minima for magnified scale of the wavelength ranging from 900 to 1100 nm

Figures 6a and 6b show, respectively, the maximum reflectance and the average of the reflectance maxima as a function of wavelength for a rough layer thickness of t_1 = 50 nm and varying glass substrate thickness t_2 in the range of 45 to 160 μm. It can be concluded from Figures 6a and 6b that by keeping t_1 constant the curve feature remains almost the same for all substrate thickness t_2 for the wavelength in the range of 300 nm to 1100 nm. The average value of the reflectance maxima shown in Figure 6b indicates an almost constant plateau with a level of statistical significance lower than 10%. The error bars were obtained from the standard deviation of the reflectance-maxima average.

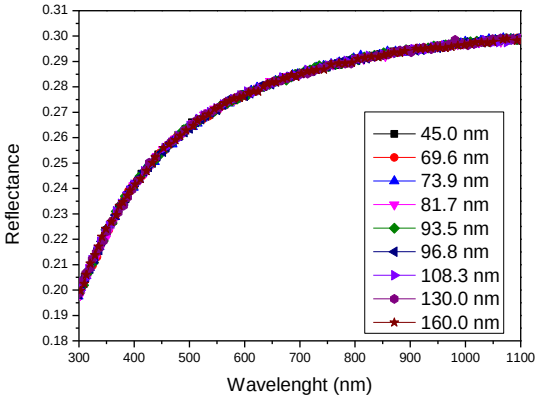

(a)

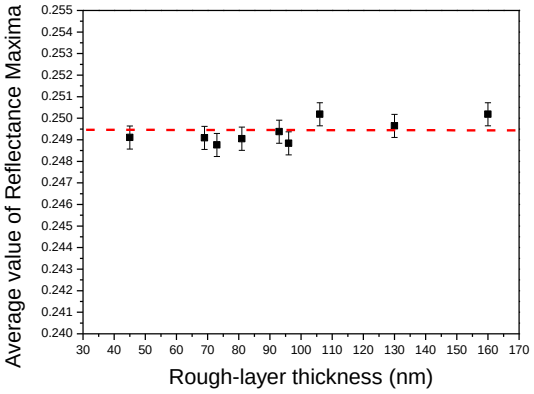

(b)

Figure 6 – Maximum reflectance as a function of wavelength (a) and average value of reflectance maxima as a function of the glass-coverslip thickness (b) for a rough layer with thickness t_1 = 50 nm and glass substrate thickness t_2 varying in the range of 45 to 160 μm.

To investigate the influence of the rough-layer thickness, it was varied in the range of 50 to 200 nm while keeping the glass substrate thickness fixed at 81.70 μm. For this

condition, Figure 7 shows that interference fringes were observed and there was substantial variation in the maximum and minimum values as a function of the rough-layer thickness in the range of 50 to 300 nm, compared to the previous case shown in Figure 6. This behavior was expected and has shown that the lower thickness of the rough layer strongly influences the envelope of the interference fringes, which was attributed to its lower thickness compared to the glass-substrate thickness, a condition analogous to the ones reported in the literature for thin transparent films deposited on silicon substrates. [18].

Figure 8a shows the maximum reflectance as a function of the wavelength extracted from the curves in Figure 7 for a glass substrate with a thickness of 81.7 µm and rough-layer thickness of 50 nm, 100 nm, 150 nm, 200 nm, and 300 nm. The case of 300 nm is not shown in Figure 7, but it was included in Figure 8a for comparison purposes in the following.

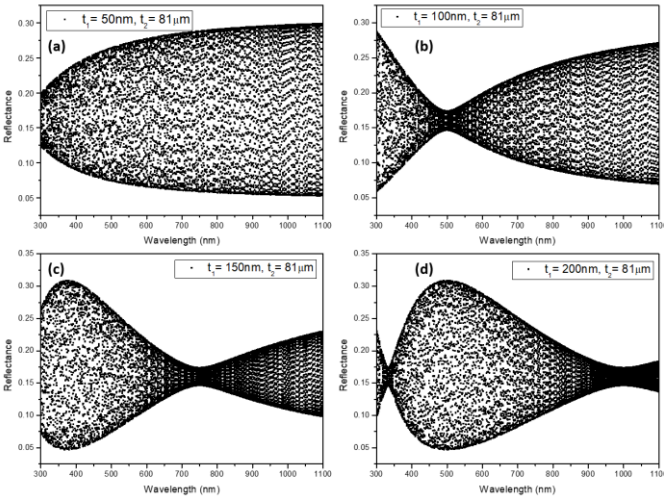

Figure 7 - Reflectance as a function of wavelength for the glass substrate with fixed thickness t_2 = 81.7 µm and rough layers with thicknesses of t_1 = 50 nm (a), 100 nm (b), 150 nm (c), and 200 nm (d).

Figure 8b shows the average value of the reflectance maxima as a function of the wavelength, extracted from the curves in Figure 8a. Although the average of the maxima at 100 nm is close to the lowest value, all the average values remained in the range of 0.228 to 0.249 considering the rough-layer thickness varying in the range of 50 to 300 nm.

For one-dimensional numerical simulation with COMSOL software for the three-layer system immersed in air considering the air/rough layer/glass on thick silicon wafers (5 mm), It was assumed the real and imaginary parts of the refractive indices, especially that of silicon (k = 0.019) which could have a significant effect. It was observed for the same simulated cases as in Figures 5 and 7 that the imaginary part of the refractive index of the layers simulated with COMSOL practically does not cause any appreciable variation of the reflectance compared to the results obtained through Equation 1. For this reason, we did not show the counterpart graphs to those presented in Figures 6b and 8b for the average value of reflectance maxima, considering a constant surface rough layer and a constant substrate thickness, respectively.

The results of reflectance maxima lower than 0.3097 in Figure 8a and reflectance-maxima average ranging from 0.242 nm to 0.252 nm in Figure 8b means that glass coverslips can enhance the conversion efficiency of light energy into electrical energy because, when covering the MOS solar cells, they can lower the surface reflectance. This is the case of indoor MOS solar cells manufactured for energy harvesting as described in the Experimental since the flat exposed silicon with a thin layer of 1.73 nm in Figure 2 presents reflectance in the range 0.65 to 0.32 for wavelength varying from 300 nm to 1100 nm according with the COMSOL simulations as shown in Figure 3, which is higher than 0.3097 in all the range of the wavelength studied for the average value of the Reflectance Maxima.

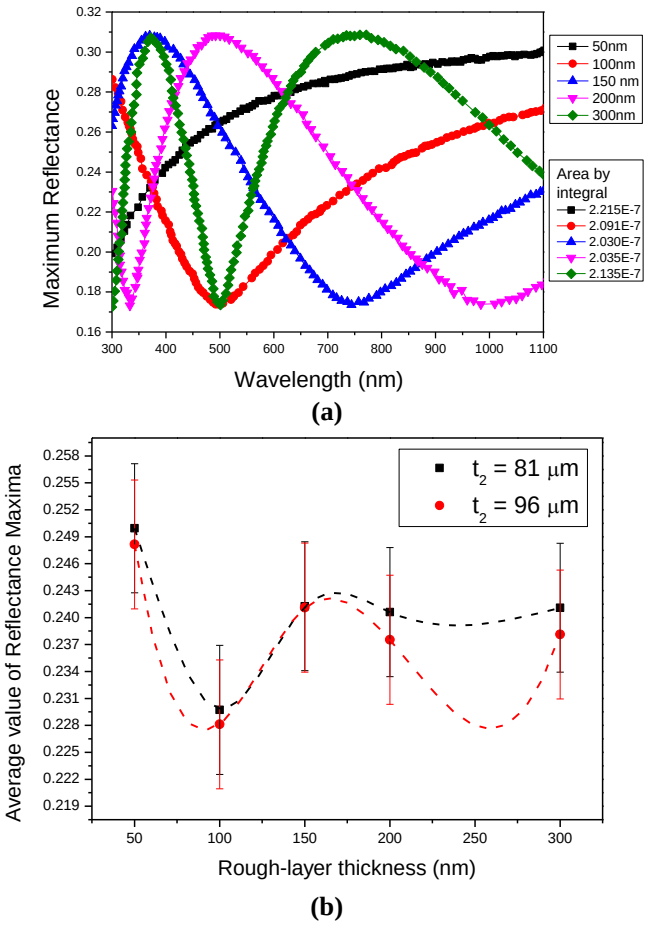

Figure 8 - Maximum reflectance as a function of wavelength (a) and average value of reflectance maxima as a function of the rough-layer thickness (b) for a glass substrate with thickness t_2 of 81.7 µm and rough-layer thickness varying in the range of 50 to 300 nm.

In order to corroborate the improvement in conversion efficiency in accordance with the prediction of the simulated results here presented, Al(200nm)/SiN_xO_y(1.73nm)/ p-Si MOS solar cells were covered with the glass coverslips, and they were illuminated with an incident power density of 11.7 mW/cm^2 from halogen lamps at 4100 K as described in Experimental.

Figure 9 shows the typical experimental current density x gate voltage (JxV_G) and calculated power density x gate voltage (PxV_G) curves of a MOS PV cell with gate fishbone geometry of 100 µm x 150 µm illuminated with an incident power density of 11.7 mW/cm^2 from a halogen lamp at 4100 K without glass coverslips. For this condition, Figure 9 shows the short circuit current density (J_{SC}), the open circuit voltage (V_{OC}) and the maximum power density (P_{max} = max [PxV_G]). Also, the fill factor (FF) and the conversion

efficiency ($\eta = P_{max}/P_{in}$) were calculated from Equations 4 and 5, respectively, where the incident power density P_{in} was obtained in mW/cm^2 from Equation 6.

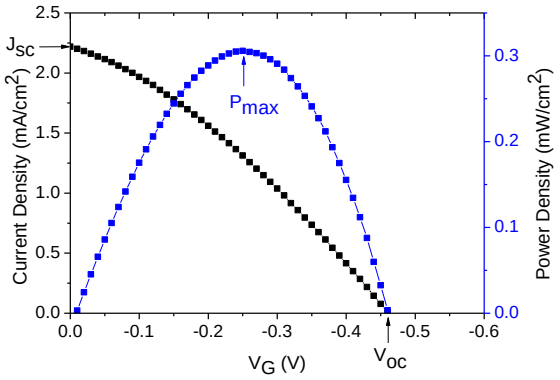

Figure 9. Typical experimental current density x gate voltage (JxV_G) and calculated power density x gate voltage (PxV_G) curves of a MOS PV cell with gate fishbone geometry of 100 µm x 150 µm illuminated with an incident power density of 11.7 mW/cm^2 from a halogen lamp at 4100 K and without glass coverslips.

Table I shows the extracted J_{SC}, V_{OC}, P_{max}, FF and η using glass coverslips with thickness of 69.6, 73.9, 81.7, 93.5, 96.8, 108.3 and 130.0 µm obtained as detailed in the Experimental. It is noteworthy that the energy conversion efficiency η increases when any coverslip is positioned onto the surface of the MOS solar cell. In particular, the as-received coverslip (~ 130 µm) promotes an increase of η from 2.63 to 3.36%. In this case, the higher the total reflectance, the lower the power transmission and, as a result, the generation current is lower in the MOS photovoltaic cell.

TABLE I. EXTRACTED J_{SC}, V_{OC}, FF, PMAX AND η

Glass Thickness (µm)	J_{sc} (mA/cm^2)	V_{oc} (V)	FF (%)	Pmax (mW/cm^2)	η (%)
without glass	2.20	0.432	32.40	0.308	2.63
69.9	2.71	0.435	30.37	0.358	3.06
73.9	3.49	0.454	27.96	0.443	3.79
81.7	4.30	0.497	28.22	0.603	5.15
93.5	3.07	0.486	27.81	0.415	3.55
96.8	4.01	0.503	27.71	0.559	4.78
108.3	4.18	0.474	26.70	0.529	4.52
130.0*	3.13	0.446	28.15	0.393	3.36

* as-received glass coverslip without any processing in BOE.

In addition, the increase of the substrate thickness from 69.9 µm means an increase of η till a maximum value of 5.15% for glass thickness around ~80 µm as depicted in Table I, and then η tends to decrease for higher glass thickness. That behavior can be explained considering the results indicated in Figure 7. Although the reflectance should not vary with the glass thickness as concluded from Figure 7a, the process in BOE during time intervals in the range of 1 to 8 h may mean a progressive thickness increase of the surface rough layer and, as a result, a minimum reflectance could be achieved around 100 nm followed by an increase of the reflectance for higher thickness as shown in Figure 7b.

Therefore, the thickness of the rough surface in Figure 7b are good estimates explaining the experimental results in Table I for the energy conversion efficiency η that follows the average value of the reflectance maxima. For non-rough samples as shown in Figure 4, the reflectance maxima are constant and lower than the silicon reflectance in the range of 300 nm to 1100 nm, which is also consistent with the higher energy conversion efficiency observed compared to the case without coverslip in Table I.

On the other hand, the open circuit voltage (V_{oc}) and the short circuit current density (J_{sc}) are well correlated by the following expression [9]:

$$V_{oc} = n\frac{kT}{q} ln\left(\frac{J_{sc}}{J_o} + 1\right) \quad (4)$$

where "n" is the ideality factor, which is primarily influenced by the gate dielectrics thickness that was 1.73 nm, *k* is the Boltzman constant (k = 8.617x10^{-5} eV/K), T is the temperature in Kelvin, q is the elemental charge (q = 1.609x10^{-19} C) and J_o is the dark current density, an approximately constant value for 1.73 nm gate dielectrics ($J_o \approx 3.9x10^{-7}$ A/cm^2).

Thus, it was shown for 81.7 µm glass coverslips that the energy conversion efficiency almost doubled (~95%) compared with the MOS solar cell without any coverslip. In addition, for the as-received coverslips (130 µm thick), it was observed an improvement of ~27% in the energy conversion efficiency.

CONCLUSIONS

Glass coverslips were found to enhance the conversion efficiency of light energy into electrical energy for MOS solar cells with surface reflectance higher than that of glass coverslips for indoor energy harvesting applications The best results were achieved for 81.7 µm glass coverslips on MOS solar cells in the wavelength range of 300 to 1100 nm.

The results of reflectance maxima lower than 0.309 and the average value of the reflectance maxima ranging from 0.228 to 0.249 means that glass coverslips enhance the conversion efficiency of light energy into electrical energy because, when covering the solar cells, they lower the surface reflectance below the silicon reflectance for wavelength in the range of 300 to 1100 nm.

The one-dimensional numerical simulation using COMSOL was very close to the analytical modeling of the air/surface rough layer/glass/silicon structure. The rough surface was modeled with different thicknesses in the range of 50 to 300 nm and with an intermediate refractive index between air and glass (n = 1.25). The thickness of the glass coverslips was varied in the range of 45 µm to 160 µm with a typical bulk refractive index of 1.50.

For Al(200nm)/SiN_xO_y(1.73nm)/p-Si MOS solar cells covered with glass coverslips and illuminated with an incident power density of 11.7 mW/cm^2 from halogen lamps at 4100 K. The energy conversion efficiency η increased when any coverslip was positioned onto the surface of the MOS solar cell. The as-received coverslip (130 µm) promoted an increase of η from 2.63 to 3.36%. In addition, the increase of the substrate thickness from 69.9 µm to 130 µm means an increase of η till a maximum value of 5.15% for glass thickness of 81.7 µm and, for higher glass thickness till 130 µm, the η decreased.

That behavior was explained considering that a minimum reflectance was achieved for a rough layer around 100 nm thick followed by an increase of the reflectance for higher thicknesses as pointed out by the simulations.

ACKNOWLEDGEMENTS

We acknowledge Coordenação de Aperfeiçoamento Pessoal de Nível Superior (CAPES) for the financial support.

REFERENCES

[1] J. Bouclé, D. Ribeiro Dos Santos, A. Julien-Vergonjanne "Doing More with Ambient Light: Harvesting Indoor Energy and Data Using Emerging Solar Cells" Solar vol. 3, no. 1, 2023, pp. 161-183. https://doi.org/10.3390/solar3010011.

[2] I. Mathews, S. Nithin Kantareddy, T. Buonassisi, I. M. Peters, "Technology and Market Perspective for Indoor Photovoltaic Cells", Joule, vol. 3, no 6, 2019, p. 1415-1426. https://doi.org/10.1016/j.joule.2019.03.026.

[3] M.Green, E.Dunlop, J.Hohl-Ebinger, M.Yoshita, N.Kopidakis and X.Hao, "Solar cell efficiency tables (version 57)". Prog Photovolt Res Appl. v. 29, 2021, pp. 3–15. https://doi.org/10.1002/ pip.3371

[4] W.Shockley and H.Queisser. "Detailed balance limit of efficiency of p-n iuction solar cells". *Iournal of Applied Physics*. v.32, n.3, 1961, pp. 510-519. https://doi.org/10.1063/1.1736034.

[5] R.Mccarthy and H.Hill. "The Shockley-Queisser limit and practical limits of nanostructured photovoltaics". *IEEE Photovoltaic Specialists Conference*, 2012, pp. 1663-1668. https://doi.org/10.1109/PVSC.2012.6317915.

[6] R.Har-Lavan and D.Cahen, "40 years of Inversion-Layer Solar Cells: From MOS to Conduct Polymer/Inorganic Hybrids", IEEE Journal of Photovoltaics, v. 3, n. 4, 2013, pp. 1443-1459. https://doi.org/10.1109/JPHOTOV.2013.2270347.

[7] C.Lin, B.-C.Hsu, M.H.Lee and C.W.Liu, "A Comprehensive Study of Inversion Current in MOS Tunneling Diodes", *IEEE Transactions on Electron Devices*, vol. 48, n. 9, 2001, pp. 2125-2130. https://doi.org/10.1109/16.944205.

[8] R. Hezel. "Recent Progress in MIS solar cells. Progress in Photovoltaics: Research and Applications". Progress in Photovoltaics, vol. 5, p.2, 1997, pages 109-120.

[9] D.L.Pulfrey, "MIS Solar Cells: A Review," *IEEE Transactions on Electron Devices*," v. 25, n. 11, 1978, pp. 1308-1317. https://doi.org/10.1109/T-ED.1978.19271.

[10] M. N. Watanabe, W. Chiappim Junior, V. Christiano, F. Izumi and S. G. Santos Filho. "MOS solar cells for indoor LED energy harvesting: influence of the grating geometry and the thickness of the gate dielectrics," *2019 34th Symposium on Microelectronics Technology and Devices (SBMicro)*, Sao Paulo, Brazil, 2019, pp. 1-4. https://doi.org/10.1109/SBMicro.2019.8919375.

[11] M. N. Watanabe, W. Chiappim Junior, V. Christiano, F. Izumi and S. G. Santos Filho. "Fabrication and Electrical Characterization of MOS Solar Cells for Energy Harvesting". *IEEE 33rd Symposium on Microelectronics Technology and Devices (SBMicro)*, 2018, pp. 1-4. https://doi.org/10.1109/SBMicro.2018.8511579.

[12] F. Izumi, M. N. Watanabe, B. S. Alandia, S. G. dos Santos Filho. "Impact of the gate work function on the experimental I-V characteristics of MOS solar cells simulated with the Sentaurus TCAD software". *Journal of Integrated Circuits and Systems*, vol. 19 no. 1, 2024, pp. 1-7. https://doi.org/10.29292/jics.v19i1.700.

[13] L.Q. Liu, X.L. Wang, M. Jing, S.G. Zhang, G.Y. Zhang, S.X. Dou and G. Wang, "Broadband and Omnidirectional, nearly zero reflective Photovoltaic Glass". *Adv. Mater*., vol. 24, 2012, p. 6318- 6322. https://doi.org/10.1002/adma.201201740.

[14] X. Yan, Wang, D.J. Poxson, J. Cho, R.E. Welser, A.K. Sood, J.K. Kim. and E.F. Schubert. "Enhanced Omnidirectional Photovoltaic Performance of Solar Cells Using Multiple -Discrete-Layer Tailored- and Low-Refractive Index Anti-Reflection Coatings". *Adv. Functional Mater*., vol. 23, 2013, p. 583-590. https://doi.org/10.1002/adfm.201201032.

[15] C. L. Nagendra and G. K. M. Thutupalli, "Design of three-layer antireflection coatings: a generalized approach," Appl. Opt. vol. 27, 1988, p. 2320-2333

[16] COMSOL Multiphysics® v. 5.6. www.comsol.com COMSOL AB, Stockholm, Sweden.

[17] K. Reinhardt and W. Kern. Handbook of Silicon Wafer Cleaning Technology. 2nd edition. Norvich, NY: William Adrew, 2008.

[18] B. Šantić, "Measurement of the refractive index and thickness of a transparent film from the shift of the interference pattern due to the sample rotation". *Thin Solid Films*, vol 518, 2010, p. 3619-3624.